

Flood Hazard Mapping and Risk Assessment in Narayani River Basin, Nepal

Anil Pangeni¹; Umesh Bhurtyal²

¹M.Sc. student, ²M.Sc. co-ordinator,

Master of Science in Geospatial Engineering Department of Geomatics Engineering,
Pashchimanchal Campus, Pokhara, Nepal

Madan Pokhrel³; Samrat Poudel⁴

^{3,4}Assistant Professor Department of Civil Engineering,
Pashchimanchal Campus, Pokhara, Nepal

Netra Bahadur Katuwal^{*5}

^{*5}Assistant Professor Department of Geomatics Engineering,
Pashchimanchal Campus, Pokhara, Nepal

Abstract:- Floods, earthquakes, forest fires, landslides, and other natural hazard are common in Nepal. Among them, the flood is one of the natural disasters and that occurred in the Narayani River basin. The Narayani River Basin's exposures and vulnerabilities are at danger from a flood catastrophe of this kind, hence this studies attempts to reduce and control the risk of flooding in order to better manage disasters. The factors of flood hazard, flood exposures, and flood vulnerability are investigated as part of the ward-level flood risk assessment, which aims to prevent and manage the flood disaster. The hydraulic model (HEC-RAS) for the 2018 flood event was used in this study to create the GIS-based modeling of the flood inundation maps. Additionally, it calculated the various return periods for floods in the river basin—5, 10, 25, 50, 75, and 100 years. Furthermore, the flood extent was confirmed using the flood map produced by the Google Earth Engine (GEE) using remotely sensed techniques. For Hydraulic modelling, ALOS/PALSAR Digital Elevation Model (12.5m.) spatial resolution was used. In addition, RAS-MAPPER generated the geometric data for the hydraulic modeling, which was then transferred into HEC-RAS. This data included the cross-section, flow route, streamline, and bank lines. On both sides of the river, the necessary Manning value "n" values were computed for every cross-section. The steady-flow models of the anticipated flood hydrographs were created using the hydraulic model. Google Earth Engine (GEE) flood maps generated from Sentinel-1C radar satellite data were used to validate the results for the 2018 flood events. When comparing the simulated result's flood inundation area with the remote sensing data's flood area, the overlap area for the 2018 flood event is 65%. Additionally, the flood area is verified. In addition, the hydraulic model generated flow conditions for 5, 10, 25, 50, 75, and 100 year return periods. The river basin's surface water level and flood extent are both progressively rising. In order to effectively manage and prepare for potential flood hazards in the study area, an analysis of the flood risk assessment was conducted by taking into consideration three primary factors: the flood hazard map, flood exposure, and flood vulnerability. The layers of the population, crops, schools, hospitals, and road network were all exposed to flooding, and the factors that determined flood vulnerabilities were literacy, urban area, and age

composition (less than 14 and more than 65). The higher flood risk area was found in Ward number 1, 3, 4,16,18,26 of Bharatpur metropolitan, Gaindakot municipality ward number 1 and 12, 15 of Madhyabindu Municipality.

Keywords:- Hydraulic model, Flood inundation, Flood risk, Flood exposure, Flood vulnerability, Flood hazard.

I. INTRODUCTION

Globally occurring, large-scale flooding causes massive damage, financial losses, and loss of life. With its varied terrain and riverine environments, Nepal is vulnerable to a wide range of natural disasters. Floods are one of the biggest threats to infrastructure, agriculture, and human settlements. In particular, the Narayani River Basin in central Nepal is prone to regular and severe flooding incidents. Large in scope and vital to the socio-economic life of the area, the basin requires careful planning and a strong management approach because of its susceptibility to flooding [1]. Flooding is a common occurrence in Nepal's Narayani River Basin, and it can be extremely destructive. The population, the infrastructure, and the ecosystems in the basin are all at serious risk from these floods. The development of mitigation strategies and effective disaster management depend on precise flood hazard mapping and risk assessment. In recent years, a potent method for assessing and mapping flood hazards has emerged: the integration of remote sensing and Geographic Information System (GIS) techniques[2]. The Narayani River Basin features a diverse landscape with complex hydrological processes and varying land use patterns. Conventional flood hazard assessment methods may struggle to capture the spatial variability and dynamics of flood events in this region due to their reliance on limited ground-based observations [3]. Using sensors on satellites or aircraft, remote sensing enables the collection of important data about the surface of the Earth. Inputs essential to flood modelling and hazard mapping include information on topography, land use, precipitation, and river morphology. GIS offers a potent platform for combining and analysing these various datasets, allowing for the creation of precise flood hazard maps that consider numerous spatial factors and variables[4]. Worldwide, there are various types of floods that can occur, including river, coastal, flash, and urban floods. Owing to their great exposure to and susceptibility to flooding, urban floods are

the most major and destructive type of flood risk[7]. According to historical data, the nation experienced significant flooding in many different years, including Tinau in 1978, Koshi in 1980, Tadi in 1985, and Sunkoshi in 1987, and Kulekhani in 1993. Therefore, flood control is necessary to lessen flood damage. Nepal has a vast supply of water. Nepal is drained by about 6000 rivers and rivulets. Large rivers in Nepal are perennial and are snow-fed by the high Himalayas. The middle mountains give rise to the rain-fed medium rivers. During the dry season, the small rivers with their sources in the southern slopes of the middle hills and the Siwalik have little to no flow. These tiny rivers play a significant role in the overall flood damage and sediment build-up. One thousands of these rivers have a length of 10 km or more, and 100 have a length of 160 km or more. When this continent experience heavy summer monsoon precipitation followed by a low-pressure system, the dense river channels create devastating flood events that submerge and destroy the land and infrastructures. Rapid flooding caused by intense precipitation in a low-lying location is known as a flash flood.

II. STUDY AREA

The Narayani River basin spans 82°53' to 86°13' longitude and 27°21' to 29°20' latitude in central Nepal. It is Nepal's second-largest river basin. The seven principal tributaries of the Gandaki river basin are Marsyangdi, Daraudi, Seti, Madi, Kali Gandaki, Budi Gandaki, and Trishuli. It originates from the Tibetan plateau flowing through high Himalayas of Northern Nepal toward the Ganges River in India. The basin lies in multiple districts of Nepal, including areas such as Chitawan, Nawalpur, Tanahun, Gorkha, Lamjung, and Manang. Chitwan National Park, is located in the southern part of the basin.

The study area lies in the southern part of Narayani River basin. It covers the area of 1290.62 square km. The study area is the Narayani River from the southern part of Devghat up to the Indo Nepal Boarder. The Annual maximum discharge collected from Devghat station from year 1963 to 2015 and daily discharge of year 2018 was used for our study purpose.

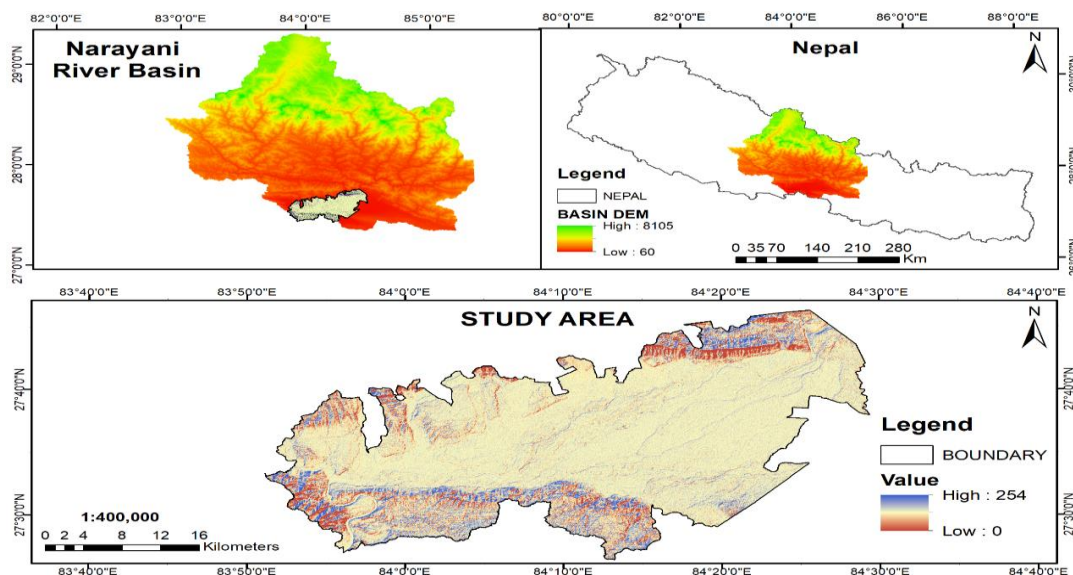


Fig. 1: Location Map of Narayani River Basin (Study area)

III. METHODOLOGY

This chapter outlines the necessary data collection sources for processing and analyzing hydrological and hydraulic models, as well as remotely sensed techniques for flood mapping and flood risk assessment.

Table 1: Data sources

S.N.	Data Type	Description	Source
1.	Digital Elevation Model	DEM ALOS PALSAR 12.5 m	https://search.asf.alaska.edu/#/ Alaska Satellite facility
2.	Land use/Cover map	Landsat 30m.	ICIMOD
3.	Discharge Data	Daily Discharge	Department of Hydrology and Meteorology, Nepal
4.	Discharge Data	Annual min. or max. (1963-2015)	Department of Hydrology and Meteorology, Nepal
5.	Flood Extent Map	Sentinel 1 Radar data	https://scihub.copernicus.eu/dhus
6.	Population	Population Density	Central Bureau of statistics, Nepal
7.	Cropland	Landsat 30m.	ICIMOD
8.	Roads	Road Network	Open street Map Contributors
9.	Hospitals, Schools	locations	Open street Map Contributors

The overall working of the study comprises of various processes as shown in figure 2 below. Modelling and simulation of flood hazard was done taking ALOSPALSAR DEM .Thus obtained flood hazard map from the simulated map for a certain discharge that took place on a certain date

was compared with the flood event map from Google Earth Engine Data repository Thus if validated flood extent map will be again used with other indexes exposure and vulnerabilities to perform risk assessment for various return period of floods.

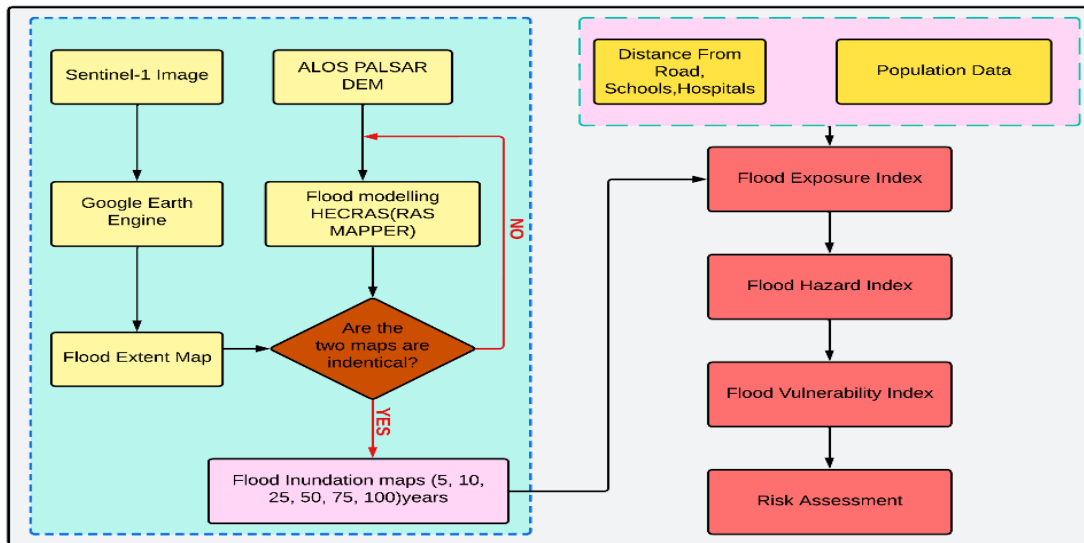


Fig. 2: Research Workflow Diagram

A. Working with Google Earth Engine

This cloud-based solution offers a large collection of satellite photos and geographical datasets that may be used with machine learning algorithms to process and analyze geospatial imagery. A wide range of users, including scientists, academic researchers, non-profit organizations, commercial enterprises, and so on, have free access to it. [15].

➤ *Remotely sensed techniques for flood detection*

Google Earth Engine (GEE) was used to perform general data processing of SAR satellite pictures. Radar satellite data were gathered via the cloud-based Google Earth Engine, which has a vast amount of satellite data accessible. The two distinct data periods—before the photos of the flood occurrences and during the flood event—are needed to compute the flood area. The raw photos were then processed for every era. Since there are more than three satellite scenes in the study region, they have been mosaicked and subset with it. The initial processing calibration was done because the scenes were at varying incident angles and relative brightness levels. This phase is crucial for the quality of SAR data. Multilooking processing will lessen the noise and pixel size inaccuracies present in the satellite outputs. With nominal image pixel size, the images will seem better. Speckle reduction processing is more successful in reducing the amount of speckle at blurred features or in lowering the resolution in the condition. Geometric correction also involved deskewing and terrain adjustment, which had to be completed prior to processing because of the differing Doppler times in the landscape. Following the processing of the two distinct satellite image periods, the flood region was extracted from the data of the pre-flood period by deducting during the flood event, particularly during the flood peak phase.

B. Working with HEC-RAS and RAS-Mapper

HEC-RAS was used for running 1-D steady flow. When flow characteristics, such as the discharge at a section, remain constant throughout time, the flow is said to be in a steady state in an open channel. Open channel flow should be regarded as unstable if the time-varying variation in flow state poses a significant risk. When the depth of the channel is constant throughout, the state of steady flow in an open channel system is referred to as steady uniform flow. On the other hand, when the depth of flow varies over the channel's length, the flow is referred to as a steady varying flow. Steady, uniform flow is the fundamental flow type that is discussed in open channel hydraulics. Additionally, varied flow might vary either quickly or gradually. The depth of flow changes suddenly over a relatively short space with rapidly shifting flow. [16].

➤ *1-D Steady flow model Development*

Floodplain mapping is done in two steps: step 1 is processing data from the RAS mapper, and step 2 is running the HEC-RAS model. HEC-RAS 6.4.1 was initially downloaded. After creating a shape file of the Narayani River basin—a critical parameter for a RAS Mapper—the case study's area was geo-referencingd. The Digital Elevation Model (DEM) image was utilized for both the mapping and the classification of the flood's magnitude. ALOS PALSAR DEM with a resolution of 12.5 m was employed. HEC-RAS's geometry includes details on flow routes, cross-sections, river banks, roughness coefficients, and other features. The HEC-RAS RAS mapping tools were used to build the river geometry, including the centerline, bank line, flow path line, and cross-section. The main water flowing channel's Manning's roughness coefficient was determined to be 0.035, while the upper and lower portions' values were 0.06 and 0.05 for the right and left overbank, respectively. [17]. 1D steady flow simulation

under subcritical flow regime was used to do the flood study. Using the Gumbel Distribution Method, flood values for the 5, 10, 25, 50, 75, and 100 return periods were determined. The steady flow data was obtained using these flood values as well as appropriate boundary conditions. Only the downstream end of the river's boundary condition was defined because the chosen flow regime was subcritical. It was delineated by the river bed's usual depth, which is determined by its slope. The software predefined the boundary condition at the junction. Following the system's simulation in HEC-RAS, depth, velocity, and elevation of the water's surface were measured and displayed in the RAS-mapper window.

C. Flood Frequency Analysis

Equation of hydrologic frequency analysis by chow(1951) was used to compute value of flood for return period 'T'[9].For this purpose Gumbels' method was used to calculate the value of Frequency Factor 'K'[11].

$$X_T = \bar{X} + k \sigma \quad \text{(Equation no 1)}$$

Where,

X_T = Value of flood for return period 'T'

\bar{X} = Mean value of flood

K= Frequency Factor

σ = Standard Deviation

Based on this equation, Gumbel's Method was derived

For calculating Frequency Factor 'K'

$$K = \frac{Y_T - \bar{Y}_n}{S_n}$$

Where $Y_T = -\ln(\ln(\frac{T}{T-1}))$

\bar{Y}_n = Mean reduced variant

S_n = Standard deviation of that reduced variant

D. Flood Risk Assessment

The vulnerabilities of people and their properties, as well as the natural flood hazards in the area, must be taken into consideration in order to comprehend the causes of the prospective flood disasters. It also explained how the three main processes of flood hazard, flood exposure, and flood vulnerability are used to calculate the expected damage caused by the flood[18]. Typhoons and other heavy rainstorms typically increase the risk of flooding, but storm surges and dyke breaches are also common in a given location [19]. The flood hazard map, which is derived from the hydrologic and hydraulic model modelling, is taken into account in the risk assessment for flooding. Additionally, open-source data, government office statistics, satellite imagery computation, and other sources will be utilized to apply the information to maps of flood susceptibility and exposure. Figure 3 illustrates the comprehensive procedure for creating the flood risk assessment map.

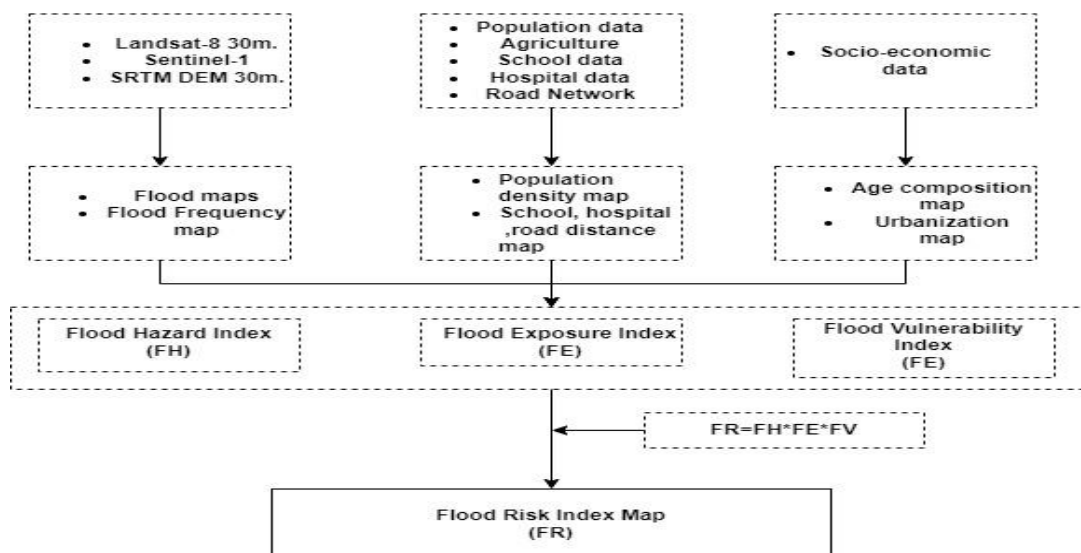


Fig. 3: Flowchart of Flood Risk Map

In risk assessment, the various sources of datasets are considered such as satellite-derived datasets, flood inundation model, open-source data, field observed data from the government (DMH), aerial statistical data and so on. The flood risk map is calculated using Equation:

$$FR = FH \times FE \times FV \quad \text{(Equation no 2)}$$

➤ **Preparation of Flood Exposure**

Exposure is defined as the value of vulnerable properties divided by the entire value of human properties. Depending on the values at the place in the flood-prone

area, it might occur. Owing to varying interpretations of susceptibility, certain studies identify exposure as a direct risk factor in the particular analysis. For this study, Ward population, Distance from road, Distance from hospital, Distance from school, Cropland, Urbanization are taken as the factors that affect the flood exposure and calculated as:

$$FE = Wp * \frac{(C + U + Sd + H + Rd)}{5} \quad \text{(Equation no 3)}$$

Where, Where FE is flood exposure, Wp is population data, C is the crop, Sd is school distance, Hd is hospital distance, and Rd is road distance.

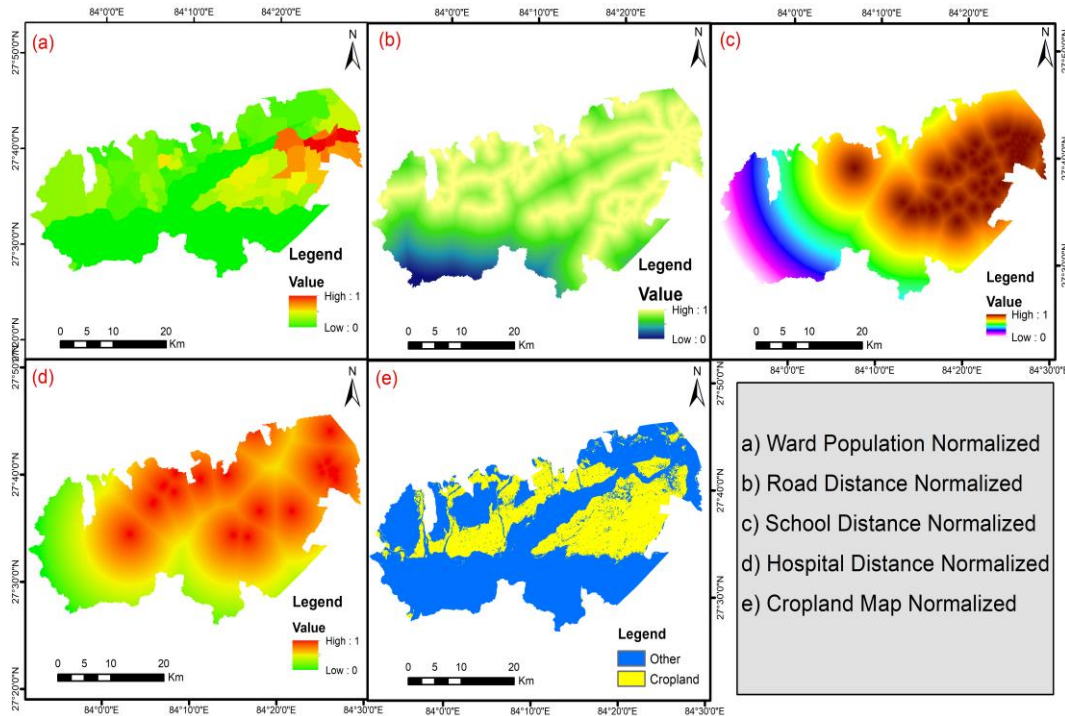


Fig. 4: Factor for preparation of Flood Exposure Map

➤ Preparation of Flood Vulnerability

The degree of loss (from 0% to 100%) resulting from the destructive phenomena, i.e., the exposure of people and infrastructure to floods and the elements' sensitivity to flood damage, is known as the flood's vulnerability. For this study, Population of age below 14, Population of age above 65, Literacy and Urbanization are taken as the factors that affect the flood Vulnerability and calculated as:

$$FV = \frac{A(<14) + A(>65) + U + L}{4} \quad \text{(Equation no 4)}$$

Where, FV is vulnerability, A (<14) is age range (Less than 14-year-old), A (65<) is age range (more than 65-year-old), U is urbanization, and L is literacy (more than 25) [20].

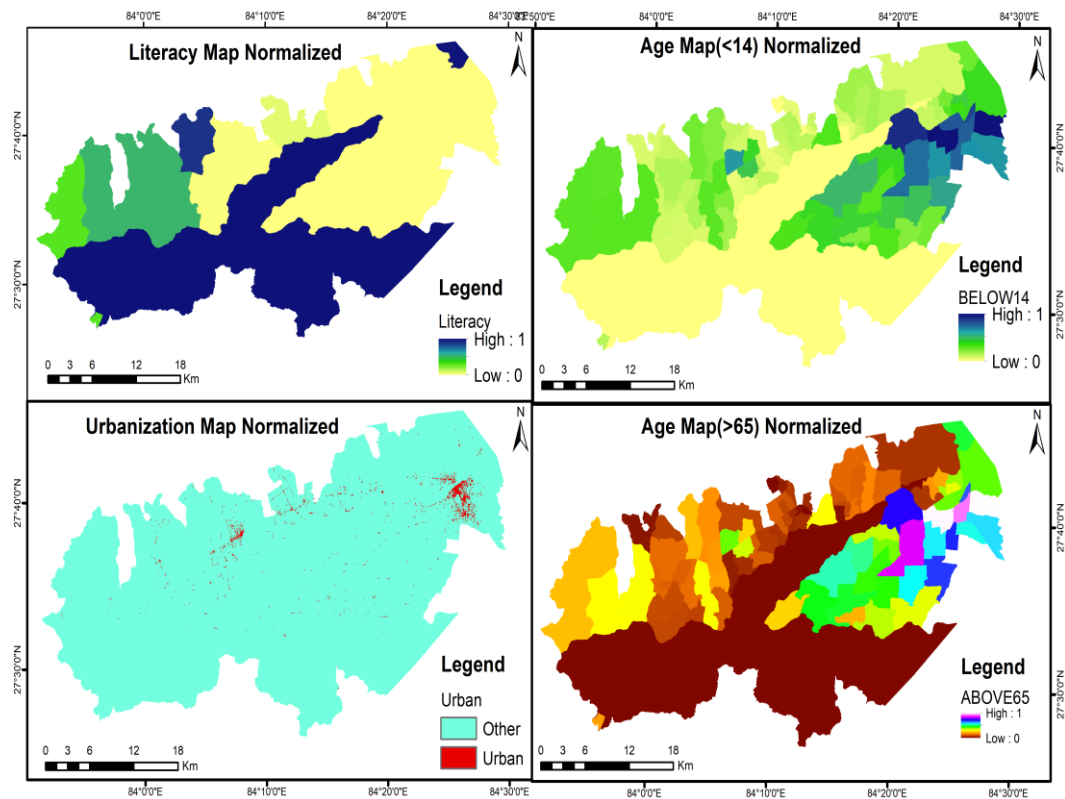


Fig. 5: Factor for preparation of vulnerability Map

IV. RESULT AND DISCUSSION

A. Flood hazard mapping

An analysis of flood danger maps was conducted for a subset of the 2018 flood occurrences. First, a flood surface model was created by exporting the cross-section and water

level (flood) profile data that were simulated in HEC-RAS into the GIS platform. The seven groups of flood inundation depth—< 2 m, 2.1-4.0 m, 4.1-6.0 m, 6.1-8.0 m, 8.1-10.0 m, 10.1-12.0 m, and > 12.0 m—were used to categorize the depth of the flood event.

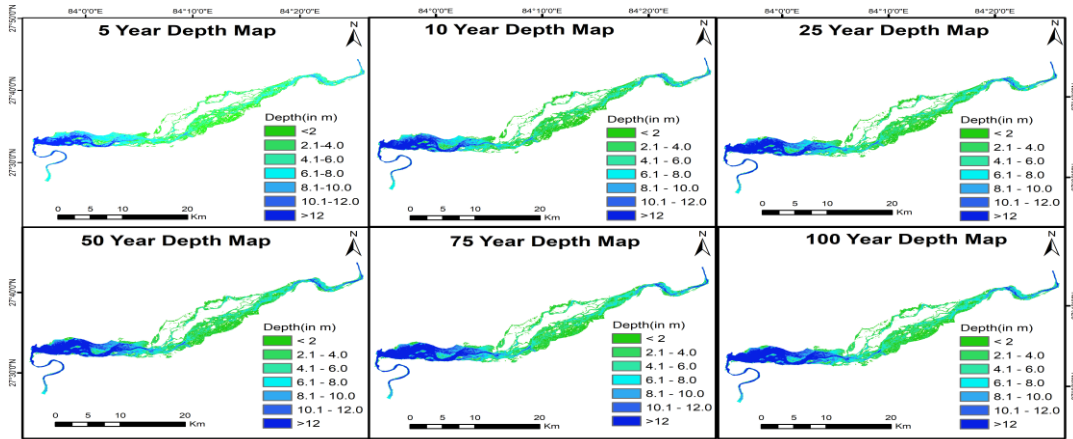


Fig. 6: Flood Hazard Map

For the flood hazard maps, the various return times of 5, 10, 25, 50, 75, and 100 years were computed. The flood's depths and extents are progressively raised in accordance

with the recurring interval for 5, 10, 25, 50, 75, and 100-year return periods, as shown in Table II.

Table 2: Flood inundation area and depths of the 5, 10, 25, 50, 75 and 100-year flood return periods

Depth (m)	Area (km ²)					
	5-Yr	10-Yr	25-Yr	50-Yr	75-Yr	100-Yr
< 2.0	37.35	35.92	33.13	30.87	29.61	28.61
2.1 - 4.0	28.50	29.27	31.12	32.00	32.46	32.92
4.1 - 6.0	20.83	20.73	21.28	22.03	22.38	22.39
6.1 - 8.0	1.355	15.47	14.53	14.09	14.22	14.57
8.1 - 10.0	10.85	11.30	12.79	12.97	12.28	11.80
10.1 - 12.0	8.492	9.42	9.80	10.51	11.01	11.33
> 12.0	16.56	21.09	27.37	31.71	34.44	36.28
Total Area (km ²)	136.96	143.23	150.038	154.217	156.456	157.929

The research utilized remote sensing techniques, specifically Sentinel-1 satellite data, to extract flooded areas during flood events. The aim was to validate flood areas in the study. The study compared results from a flood inundation map generated by the HEC-RAS model with

flood-prone areas extracted from Sentinel-1 data for the 2018 flood events. The overlap between the simulated map and Sentinel-1 data showed a 65% match, indicating reasonably good validation for the simulated maps. The comparison is illustrated in Figure 7.

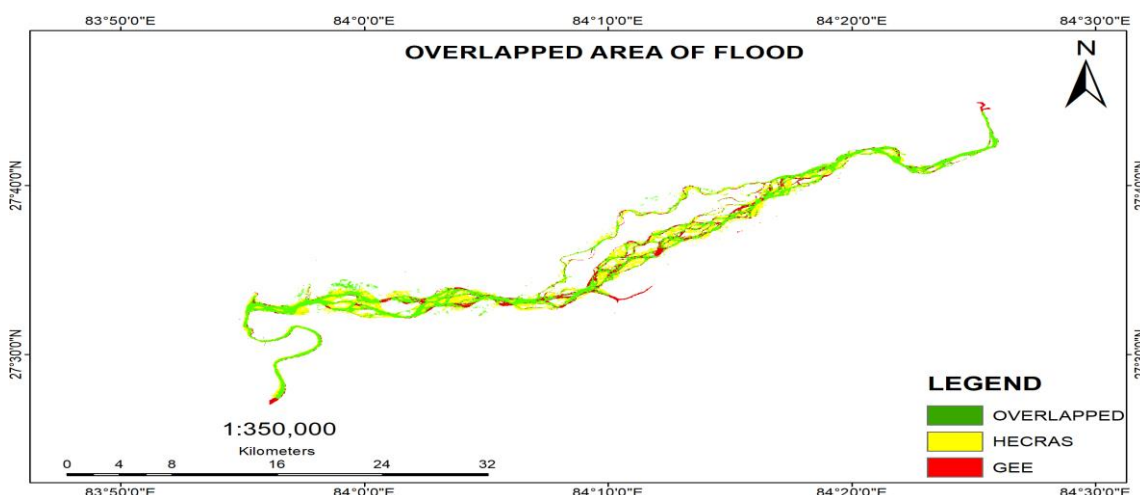


Fig. 7: Overlapped area of 2018 Flood

The flood exposure map, as seen in Figure 8, was computed based on the several variables that may be exposed in the Narayani river basin, including population, agriculture, school and hospital locations, and road networks. The research area's north eastern sector saw increased flood exposures due to the densely populated and farmed areas, particularly in the Bharatpur Townships. Furthermore, it is crucial to take the flood risk area into account while assessing flood Vulnerability. The four

characteristics that are considered to be potential flood vulnerabilities in this study are the age composition of old and kid people (those who are over 65 and those who are under 14), literacy, and urban area. The Bharatpur ,Gaindakot Townships were identified as having high flood susceptible zones based on the results of the investigation. On the other hand, as Figure 8 illustrates, the area south of the watershed was investigated as low that is the area of Chitwan national park.

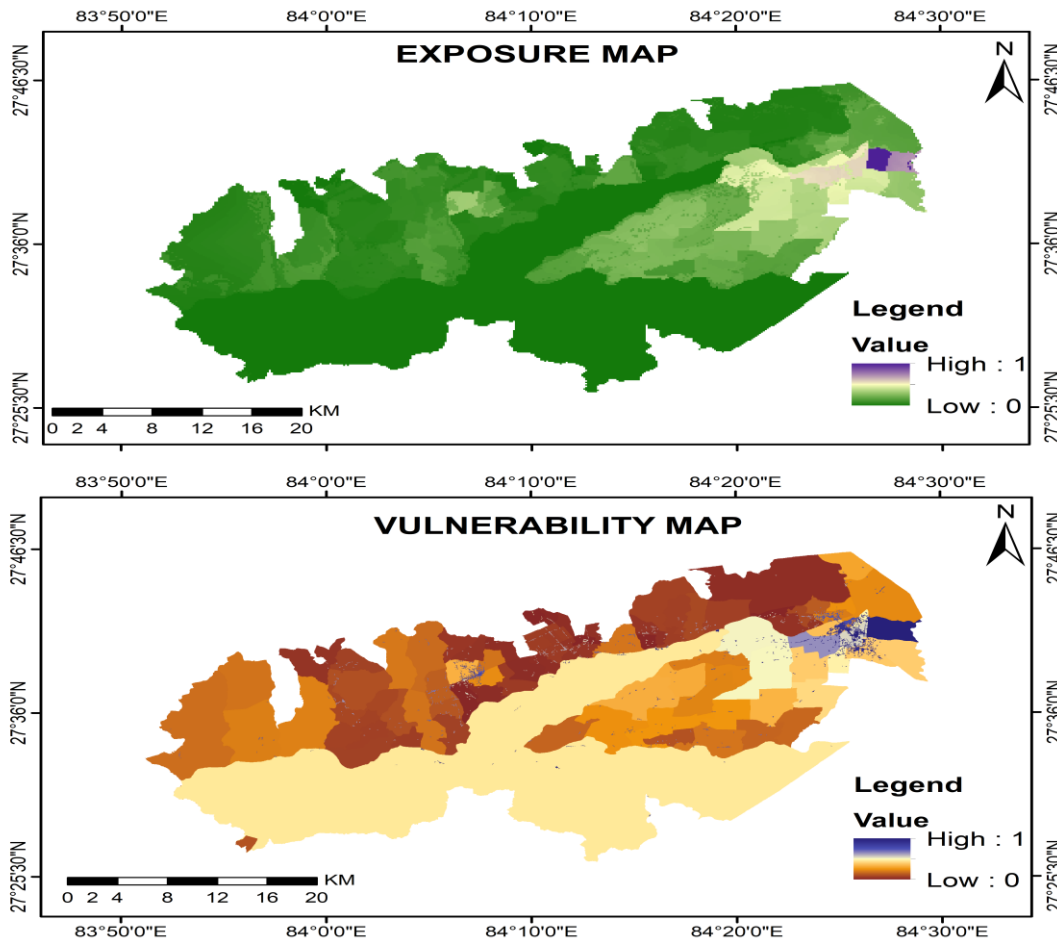


Fig. 8: Flood exposure and Vulnerability Map

B. Flood Risk Assessment

Flood exposure, flood susceptibility, and flood hazard were taken into account when assessing flood risk. The flood hazard map utilized in this flood risk assessment was created using the model, which was simulated for the 5, 10, 25, 50, 75, and 100-year return period. It was classified into seven classes according to the flood depth. The flood exposure map, as seen in Figure 7, was computed based on the several variables that may be exposed in the Narayani river basin, including population, agriculture, school and hospital locations, and road networks. The research area's north eastern sector saw increased flood exposures due to the densely populated and farmed areas, particularly in the Bharatpur Townships. Finally, the flood risk assessment was computed by taking into consideration the flood hazard, flood exposure, and flood vulnerability—three

major criteria that were computed independently in the sections that before this one. The link between the exposure classes, flood depth hazard classes, and land use vulnerability classes in a specific location defines flood risk. In order to do this, the flood depth grids of various year return period floods are overlaid with the exposure and vulnerability classes to create the flood risk maps. In light of exposure, vulnerability classes, and water depth hazard classes, this illustrates possible flood locations. In the study, it was found that the areas of Bharatpur metropolitan(1,3,4,6,18,26),Gaindakot(1),Madhyabindu(12, 15) , and some parts of Binayetriveni ward 1 near the main channel are at a high risk over 100 year return period of flood. Similarly, areas of Gaindakot (7), Madhyabindu (2,5,4), Bharatpur (28)and kawasoti(17) are at a medium risk over 100 year return period of flood.

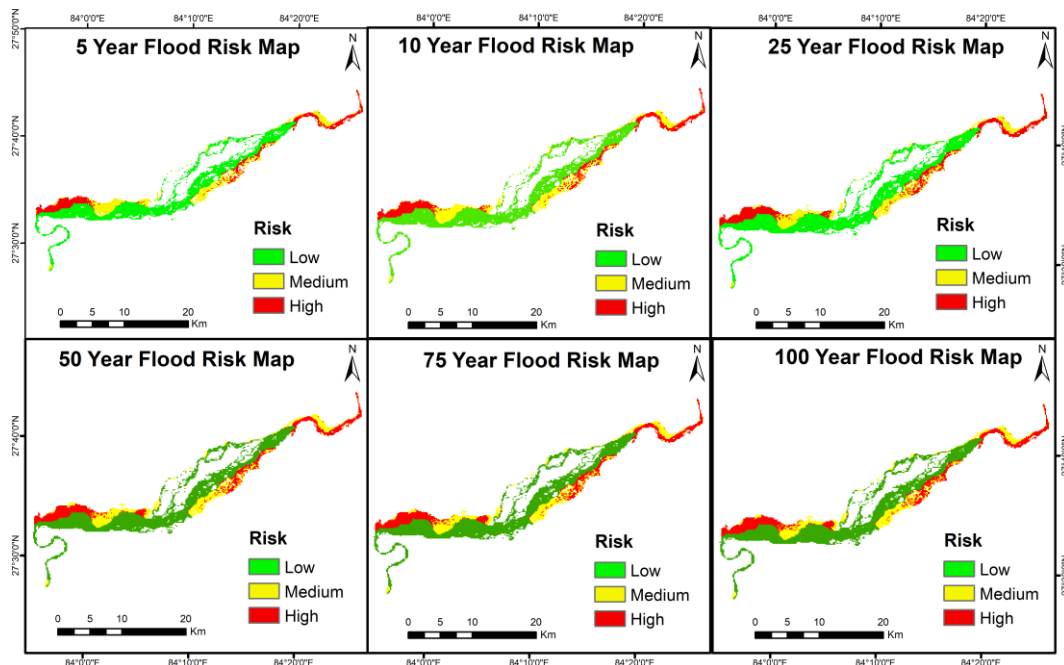


Fig. 9: Flood Risk Map

There are few hydrodynamic model and GIS applications for floodplain analysis and risk mapping in countries like Nepal, where there is also a serious deficiency of topographic, hydrological, and geometric river data. Since there is significantly more variance in river flows and no regulation of any kind in place, the scenario with river floods in Nepal is likewise quite different. The river banks and boundary lines are not well defined, and there are relatively few flood control features like spurs and dikes. As a result, many additional sets of limitations apply to the research and modelling of floodplains. This study offers a method for carrying out a comparable investigation within these limitations. The two main programs utilized for this investigation were ArcView GIS and HEC-RAS. The RAS MAPPER plugin made it easier for ArcView GIS and HEC-RAS to interchange data. A number of necessary factors were carefully taken into account throughout the model run in HEC-RAS. The Digital Elevation Model (DEM) picture was utilized for both the mapping and the classification of the flood's magnitude. HEC-RAS's geometry includes details on flow routes, cross-sections, river banks, roughness coefficients, and other features. For return period "T," the value of the flood was calculated using Gumbel's approach. Thus computed data were used in flood inundation mapping for floods of various return period. Obtained inundation maps were validated with the flood area map obtained from GEE. Flood Risk Assessment was done keeping account on three aspects i.e. Hazard, exposure and vulnerability. Flood-prone locations were identified through risk assessment. Vulnerability was measured taking in account the people age group below 14 and above 65, urbanization and literacy. Exposure was measured taken in account the total population, cropland, urban area, and distance from roads, schools and hospitals. Risk associated with floodwater depths and the time it takes for floods to recur. The seven groups of flood inundation depth—< 2 m, 2.1-4.0 m, 4.1-6.0 m, 6.1-8.0 m, 8.1-10.0 m, 10.1-12.0 m, and > 12.0 m—were used to

categorize the depth of the flood event. It was found that flood water depth >10 m increased with increased flooding intensity, and flood water depth <2 meter decreased with increased flooding intensity. A significant danger to the crop field with water is shown by the generated flood risk maps. Since these regions are the most vulnerable to flooding in river floodplains, further thought needs to be given to flood protection.

V. CONCLUSION AND RECOMMENDATION

A. Conclusions

The main cause of flooding in the Narayani River basin is riverine floods, which are brought on by intense rainfall and additional conditioning factors like topography, discharge rate, and so on. Additionally, a simulation of design flood hydrograph was run for return periods of 5, 10, 25, 50, 75, and 100 years. The flow conditions of the various river return periods that were examined in the HEC-RAS model were calculated using the observed water level data. Sentinel 1 satellite data for the year 2018 was used to validate the flood area in the river basin. The assessment of flood risks is critical to the management of flood risks. But because flood exposures, vulnerabilities, and hazard zones must all be taken into account, an enormous number of datasets are needed. A flood hazards map based on the 5, 10, 25, 50, 75, 100-year return period flood estimated by HEC-RAS was used in this work. In order to create the flood exposure map, the population density, cropland, locations of schools and hospitals, and road network were utilized and transformed into raster format. Furthermore, a flood vulnerability map was generated using the age composition and urban area datasets. The hazard, exposure and vulnerabilities are normalized and used to calculate the flood risk over the study area. The risk zones were classified into low, medium and high risk zones.

B. Recommendations

In light of the research's findings, I would like to suggest the following:

- High resolution topographic data is recommended to accurately reflect the topography of the floodplains for modelling flows in overbanks.
- Geometric data is important for the hydraulic model, in particular the cross-section survey can be carried out in the field for the better outcomes of flood modelling.
- Flood studies must to be taken into account when estimating future floods using various time series analysis.
- For an improved assessment of flood risk, the data grid containing recent population density information for flood exposure should be used.
- For future flood risk assessment, LULC change dynamics, future socio- economic changes should be considered.
- For better presentation and increased accuracy in the flood study of the entire river basin, 2D hydrodynamic models will be suggested.

REFERENCES

- [1]. K. Gautam and K. Dulal, "Determination of Threshold Runoff for Flood Warning in Nepalese Rivers," *J. Integr. Disaster Risk Manag.*, vol. 3, no. 1, pp. 125–136, 2013, doi: 10.5595/ijdrim.2013.0061.
- [2]. X. Wang and H. Xie, "A review on applications of remote sensing and geographic information systems (GIS) in water resources and flood risk management," *Water (Switzerland)*, vol. 10, no. 5, pp. 1–11, 2018, doi: 10.3390/w10050608.
- [3]. P. A. Brivio, R. Colombo, M. Maggi, and R. Tomasoni, "Integration of remote sensing data and GIS for accurate mapping of flooded areas," *Int. J. Remote Sens.*, vol. 23, no. 3, pp. 429–441, 2002, doi: 10.1080/01431160010014729.
- [4]. K. Uddin, D. Raj Gurung, A. Giriraj, and B. Shrestha, "Application of Remote Sensing and GIS for Flood Hazard Management: A Case Study from Sindh Province, Pakistan," *Am. J. Geogr. Inf. Syst.*, vol. 2, no. 1, pp. 1–5, 2013, doi: 10.5923/j.ajgis.20130201.01.
- [5]. Journal and E. S. Vol, "FACTORS ASSOCIATED TO FLOOD RESILIENCE MEASUREMENT IN," vol. 9, no. 5, pp. 1–11, 2021.
- [6]. J. R. Santillan, J. T. Marqueso, M. Makinano-Santillan, and J. L. Serviano, "Beyond flood hazard maps: Detailed flood characterization with remote sensing, gis and 2D modelling," *Int. Arch. Photogramm. Remote Sens. Spat. Inf. Sci. - ISPRS Arch.*, vol. 42, no. 4W1, pp. 315–323, 2016, doi: 10.5194/isprs-archives-XLII-4-W1-315-2016.
- [7]. L. Tascón-González, M. Ferrer-Julía, M. Ruiz, and E. García-Meléndez, "Social vulnerability assessment for flood risk analysis," *Water (Switzerland)*, vol. 12, no. 2, 2020, doi: 10.3390/w12020558.
- [8]. P. V. Timbadiya, P. L. Patel, and P. D. Porey, "Calibration of HEC-RAS Model on Prediction of Flood for Lower Tapi River, India," *J. Water Resour. Prot.*, vol. 03, no. 11, pp. 805–811, 2011, doi: 10.4236/jwarp.2011.311090.
- [9]. Te Chow, "J a m £ | i," vol. 32, Number, no. 2, 1951.
- [10]. T. Edition, *Engineering hydrology*. 1984. doi: 10.1201/9780429094811-13.
- [11]. F. Onen and T. Bagatur, "Prediction of Flood Frequency Factor for Gumbel Distribution Using Regression and GEP Model," *Arab. J. Sci. Eng.*, vol. 42, no. 9, pp. 3895–3906, 2017, doi: 10.1007/s13369-017-2507-1.
- [12]. B. Thapa, A. Danegulu, N. Suwal, S. Upadhyay, B. Manandhar, and R. Prajapati, "Rainfall-Runoff Modelling of the West Rapti Basin, Nepal," *Tech. J.*, vol. 2, no. 1, pp. 99–107, 2020, doi: 10.3126/tj.v2i1.32846.
- [13]. K. Poudel, K. Basnet, and B. Sherchan, "IJERT-Hydrological and Hydraulic Modeling for Flood Analysis: A Case Study for Modi Catchment Hydrological and Hydraulic Modeling for Flood Analysis: A Case Study for Modi Catchment," *IJERT J. Int. J. Eng. Res. Technol.*, vol. 10, no. 08, pp. 534–544, 2021, [Online]. Available: www.ijert.org
- [14]. K. Aryal and M. Regmi, "Flood Map Delineation of Narayani River Using HEC-RAS ," vol. 8914, pp. 117–127, 2022.
- [15]. M. Amani et al., "Google Earth Engine Cloud Computing Platform for Remote Sensing Big Data Applications: A Comprehensive Review," vol. 13, pp. 5326–5350, 2020.
- [16]. L. B. Maharjan and N. M. Shakya, "Comparative Study of One Dimensional and Two Dimensional Steady Surface Flow Analysis," *J. Adv. Coll. Eng. Manag.*, vol. 2, no. c, p. 15, 2016, doi: 10.3126/jacem.v2i0.16095.
- [17]. "mannings value.pdf"
- [18]. K. Shiwaku and R. Shaw, "Disaster Prevention and Management: An International Journal Article information :," *Disaster Prev. Manag. An Int. J.*, vol. 17, no. 2, pp. 183–198, 2008.
- [19]. L. Yang, "Climate Change, Water Risks and Urban Responses in the Pearl River Delta, China," pp. 3–152, 2014.
- [20]. K. Phongsapan et al., "Operational Flood Risk Index Mapping for Disaster Risk Reduction Using Earth Observations and Cloud Computing Technologies: A Case Study on Myanmar," *Front. Environ. Sci.*, vol. 7, no. December, pp. 1–15, 2019, doi: 10.3389/fenvs.2019.00191.